IEEE Access
Multidisciplinary Rapid Review Open Access Journal

Received January 10, 2019, accepted January 30, 2019, date of publication February 7, 2019, date of current version March 5, 2019.

Digital Object Identifier 10.1109/ACCESS.2019.2897981

Carbon Heating Tube Used for Rapid Heating System

TOSHIYUKI SAMESHIMA[1], TOMOYOSHI MIYAZAKI[1,2], GO KOBAYASHI[3], TAKUJI ARIMA[1], (Member, IEEE), TOSHITAKA KIKUCHI[1], TAKUMA UEHARA[1], TAKASHI SUGAWARA[1], MASAHIKO HASUMI[1], AND IZUMI SERIZAWA[3]

[1]Graduate School of Engineering, Tokyo University of Agriculture and Technology, Tokyo 184-8588, Japan
[2]Techno Research, Ltd., Tokyo 184-0012, Japan
[3]ORC MANUFACTURING Co., Ltd., Chino 391-0011, Japan

Corresponding author: Toshiyuki Sameshima (tsamesim@cc.tuat.ac.jp)

This work was supported in part by the Japan Science and Technology Agency ASTEP under Grant AS3015022S.

ABSTRACT We report a microwave heating system with a carbon heating tube (CHT) which was made by a 4-mm diameter quartz tube filled with carbon particles and Ar gas at 1400 Pa. A 60-mm-long CHT was set in a cavity in which 2.45-GHz microwave was introduced. Via nearly complete absorption of a microwave power of 200 W by carbon in the CHT during multi-reflection of the microwave in the cavity, the CHT was effectively heated to 1279 °C at 33 s after the microwave initiation, which was observed by the radiation-type thermometer. Moreover, the control of the CHT temperature was demonstrated with a home-made proportional–integral–differential feedback circuit which regulated the magnetron power source using a signal of the thermometer. The control of temperature at 1100 °C was successfully realized. Crystallization of a 58-nm-thick amorphous silicon thin film formed on the glass substrate was demonstrated by mechanically moving the silicon sample just below the heated CHT. A high crystalline volume ratio of 0.92 was achieved. Furthermore, heating of 500-μm-thick-n-type silicon substrate implanted with 1.0×10^{15} cm^{-2} phosphorus and boron atoms with the CHT resulted in activation of the doped regions. Rectified diode characteristics were achieved.

INDEX TERMS Electromagnetic interference, heat treatment, low-microwave power electronics, PID temperature control, silicon.

I. INTRODUCTION

Thermal annealing is important to fabricate semiconductor devices such as thin film transistors (TFTs) and solar cells [1]–[7]. Activation and crystallization are achieved by heat treatment to form the pn junction and crystalline state [8]. Many heating technologies have been developed such as laser annealing, plasma jet annealing, and rapid thermal annealing [9]–[15]. We have recently proposed a combination of the carbon powder absorber with 2.45 GHz microwave irradiation as a simple rapid thermal annealing method [16], [17]. Conductive carbon is effectively heated via free carrier absorption of the electromagnetic energy with excellent thermal properties of low specific heat and high heat proof [18], [19]. It is also heated by absorption of microwave generated from the magnetron. We have found that the low packing density of carbon powders about 0.08 allows effective absorption of microwave and demonstrated carbon heating at the temperature of 1163 °C by 1000 W microwave irradiation for 28 s in air atmosphere [17]. However, there was a problem of oxidation of carbon powders by oxygen in air during heating.

In order to realize a convenient heating source, we developed a lamp of carbon heating tube (CHT), in which 2-μm-diameter-carbon powders were filled with inert gas in a quartz tube whose edges were then closed by thermal welding. The carbon powders in the CHT effectively absorb microwave and heat to a high temperature with no loss of carbon powers via oxidation [20].

In this paper, we report further development of the CHT heating system and its application. The essential concept of CHT heating system is given at first. Typical characteristic of temperature change of the CHT by microwave irradiation with a constant power is then discussed. We demonstrate CHT heating higher than 1200 °C by microwave irradiation at a low power of 200 W. Next, we report temperature control of

The associate editor coordinating the review of this manuscript and approving it for publication was Andrei Muller.

2169-3536 © 2019 IEEE. Translations and content mining are permitted for academic research only.
Personal use is also permitted, but republication/redistribution requires IEEE permission.
See http://www.ieee.org/publications_standards/publications/rights/index.html for more information.

CHTs using a home-made-proportional-integral-differential feedback (PID) circuit [21] which regulated the magnetron power source with a signal of the thermometer. The temperature control is the most important point for developing a heating system. Successful control of temperature at 1100 °C is demonstrated. We also demonstrate application of the present heating system to crystallization of amorphous silicon films with a four-inch-diameter size and activation of silicon with implanted dopant atoms.

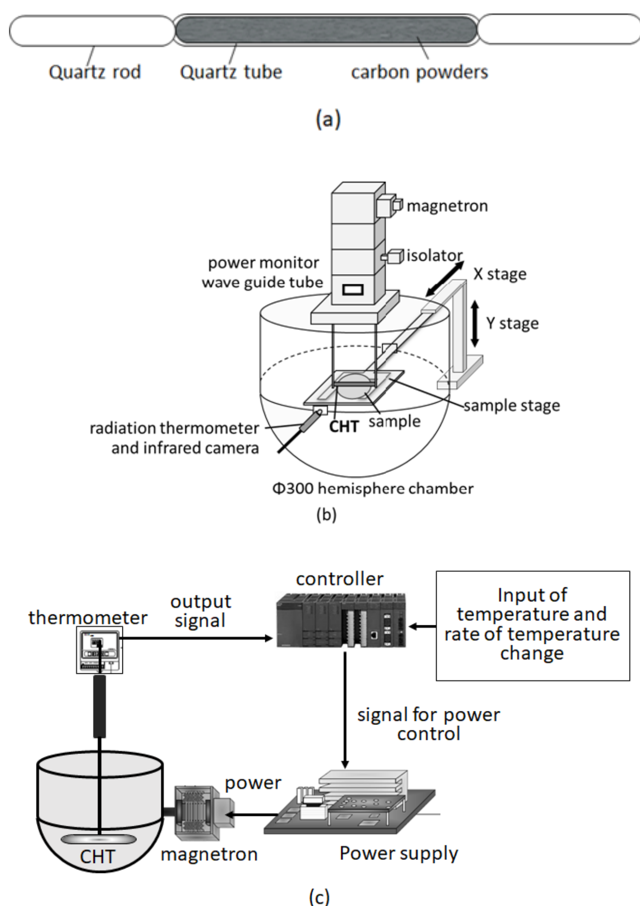

FIGURE 1. (a) Schematic image of a CHT, (b) heating system with the CHT, and (c) PID circuit to control CHT temperature.

II. EXPERIMENTAL PROCEDURES

Figure 1 shows (a) a schematic image of a CHT, (b) a heating system with the CHT, and (c) a PID circuit to control CHT temperature. Quartz tubes with 60-mm long and 4-mm inter diameter and 6-mm outer diameter were made.

2-μm-diameter-carbon powders with a 0.1-g weight were put in the quartz tubes, in which the packing density was controlled as 0.09 with an electrical conductivity of 55 S/m, which was determined by the previous work as the best value for heating [17]. After carefully evacuating air gas inside the quartz tubes by a vacuum pump under keeping carbon powders stay in the quartz tubes, Ar inert gas was filled in the quartz tube at 1400 Pa. The edges of the quartz tubes were closed by thermal welding. Two quartz rods were jointed at the edges of the CHT by thermal welding to hold the CHT. A CHT with a different length of 150 mm and carbon powders with a 0.25 g was also fabricated. The carbon is consequently heated in the quartz tube by microwave irradiation with no oxidation.

A CHT was placed in the heating system as shown in Fig. 1(b), which consists of a magnetron for generating 2.45-GHz microwave with an electrical power source, an isolator for blocking the reflectance of microwave backward the magnetron, a power monitor, an impedance matching box for reducing microwave reflectance, a wave-guide tube, and a microwave cavity made by Al metals. The Microwave generated by the magnetron was introduced to the cavity by the wave guide tube via the isolator, power monitor, and impedance matching box. The cavity had a sophisticated structure with a cylindrically upper part with a diameter of 300 mm and a spherically lower part to promote interferingly multiple reflection of the microwave in the cavity and to have the CHT effectively absorb the microwave. This designed cavity achieved to effectively close microwave power in the cavity. Those works resulted in a reflected power less than 4 W in the case of an input power of 500 W. In contrast, the power monitor gave the same value of the input and reflected power when the cavity had no CHT. The cavity completely reflected the microwave power. The CHT effectively absorbed the microwave power during the multiple reflection of microwave in the cavity. The cavity had a window port for observing light emission from CHT heated by microwave. A thermometer detecting 900-nm wavelength radiation light CHINO IR-FAS was used to monitor the temperature of the CHT in real time. The detection lower limit of the thermometer was about 550°C. An infrared digital camera was also used to observe CHT heating behavior. A mechanically moving stage was also installed in the cavity, as shown in Fig. 1(b) to move a sample just below the CHT for demonstration of heating samples by the CHT. An electrical circuit was developed to control the CHT temperature, as shown by a schematic image in Fig. 1(c). The analog voltage signal of the thermometer is monitored in real time by a PID circuit controller which was installed with a plan of temperature increasing and decreasing ratios, a target temperature and its duration in its memory in advance. The controller sent a signal to the power source of the magnetron to increase or decrease the microwave power for coinciding the CHT temperature with the initial temperature plan.

The electric field distribution in the cavity in the steady state during microwave irradiation was numerically analyzed by a simulator constructed with the three dimensional finite element moment method combined with the Cholesky decomposition [22]. The grid system of the cavity and waveguide was formed with the equilateral-triangle elements with the sides ranging from 1 to 4 mm for the numerical calculation. They were assumed as perfect electric conductor which reflects completely the microwave. The CHT grid was formed with 1-mm-side-equilateral-triangle elements. The electrical

conductivity of the CHT was set as 55 S/m according to our previous experimental investigation.

For application of the present CHT heating system to crystallization of silicon films, 58-nm-thick amorphous silicon films formed on 4-inch sized quartz glass substrates were prepared by plasma enhanced chemical vapor deposition at 300°C. The silicon film samples were heated by moving at 0.12 mm/s in the normal direction just below a 150-mm-long CHT with an inner diameter of 4 mm and a 0.25-g-carbon powders under continuous microwave irradiation at 400 W. Raman scattering and optical reflectivity spectra measurements were used to estimate crystallization properties with the crystalline volume ratio.

25-Ωcm n-type single crystalline silicon substrates with a thickness of 500 μm, a crystalline orientation of (100) and a 4-inch diameter were also prepared for demonstration of activation of implanted silicon region by the CHT heating system. The silicon substrates were coated with 100-nm-thick thermally grown SiO_2 layers by heating in a wet atmosphere at 1100°C. The ion implantation of boron atoms was conducted for the top surface of the n-type silicon substrates. The acceleration energy was set at 25 keV to obtain the peak concentration at the interface of the thermally grown SiO_2 and silicon. The total dose was 2.0×10^{15} cm^{-2}. Boron atoms at a dose of 1.0×10^{15} cm^{-2} were effectively implanted in the silicon substrates. The ion implantation of phosphorus atoms at 75 keV and a dose of 2.0×10^{15} cm^{-2} was also conducted to the rear surface. Phosphorus atoms at a concentration of 1.0×10^{15} cm^{-2} were effectively implanted in the silicon rear surface region. The silicon samples were heated by moving the sample just below a 150-mm-long CHT at 0.12 mm/s facing the boron doped surface under microwave irradiation at 400 W to heat the CHT at 1100 °C. Optical reflectivity spectra were measured to investigate the crystalline volume ratio X in the ion-implanted surface regions. The sheet resistivity was non-destructively measured by 9.35-GHz-microwave-transmittance measurement system in the dark field using the effect of the microwave absorption caused by free carrier generated in silicon substrate [22], [23]. The current density as a function of voltage was also measured via formation of Al electrodes to investigate diode characteristic.

III. RESULTS AND DISCUSSION

Figure 2 shows (a) a photograph of light emission from the 60-mm-long CHT heated by 200-W microwave irradiation for 33 s detected by the infrared camera and (b) changes in the temperature of the CHT with time during and after the 200 W microwave irradiation measured by the thermometer. Strongly blight light emission was observed at 33 s in about 40-mm long region. This indicates that heat diffusion occurred inside the CHT to make the temperature uniform in the CHT during microwave irradiation. The CHT effectively absorbed the microwave power and spatial-uniformly heated to a temperature high enough to emit blight light. The temperature increased with time in the initial stage, as shown in Fig. 2(b). This means that increase in the temperature was governed by heat capacity of the CHT. The maximum rate of temperature increase was obtained as 56 K/s. On the other hand, the increasing rate of temperature became low as the temperature increases especially in the case of the final stage of microwave irradiation. A radiation power loss caused by black-body radiation became important. A high temperature of 1279 °C was observed at 33 s. When the microwave irradiation was terminated, the temperature of CHT was rapidly decreased because of the radiation loss. The experimental maximum temperature of the 60-mm-long CHT increased from as 932 to 1279 °C as the microwave power increased from 100 to 200 W for a 33-s irradiation case. These results indicate that a rapid heating system with a low power consumption was realized.

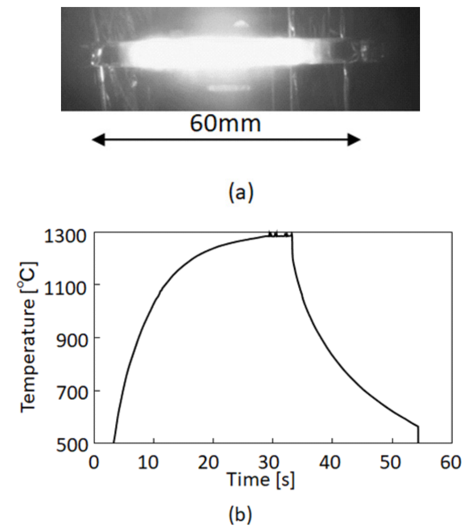

FIGURE 2. (a) Photograph of light emission from the 60-mm-long CHT heated by 200-W microwave irradiation for 33 s and (b) changes in the temperature of the CHT with time during and after the 200 W microwave irradiation.

Figure 3 shows calculated cross-sectional electric field distributions in the cavity (a) without CHT, (b) with the CHT placed at the central region of the cavity, and (c) with the CHT described in detail lower than 9 kV/m when the 200 W microwave was continuously introduced in the cavity. The cavity and CHT surface outlines were traced by sold black curves. The calculation resulted in the standing wave of the electric field in the both cases because of the three dimensional Fresnel interference effect observed in the cavity. The numerical calculation resulted in a high electric field existed in the cavity. The intensity distributed from 1000 to 6000 kV/m, as shown in Fig. 3(a). In contrast, electric field was very low in the case of the cavity with the CHT. Their intensity was lower than 10 kV/m in the cavity space. On the other hand, it was high of ranging from 50 to 80 kV/m around the CHT, as shown in Fig. 3(b). The electric field ranged from 1 to 6 kV/m in the most of region of the cavity, as shown in Fig. 3(c). It was reduced to at least 0.1% of the initial intensity of the cavity space without CHT. These calculated results indicate that the cavity effectively accumulated

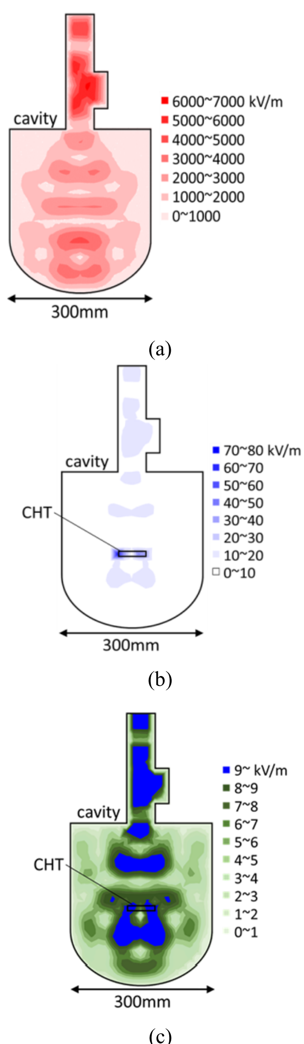

FIGURE 3. Calculated distribution of the electric field intensity in the cavity (a) without CHT. (b) with the 60-mm-long CHT with an electrical conductivity of 55 S/m placed in the central region of the cavity, and (c) with the CHT described in detail lower than 9 kV/m when the 200 W microwave continuously was introduced into the cavity.

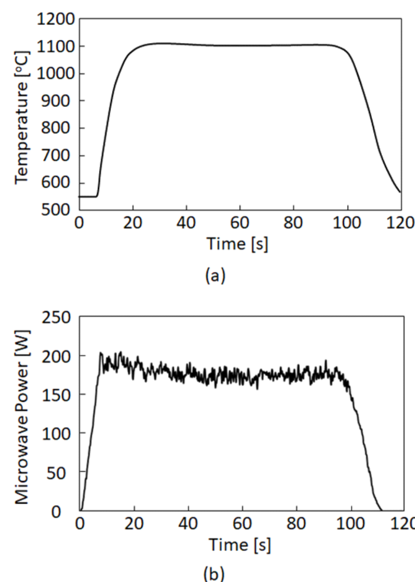

FIGURE 4. (a) Temperature change of the 60-mm-long CHT controlled using the PID circuit and (b) change in the microwave power.

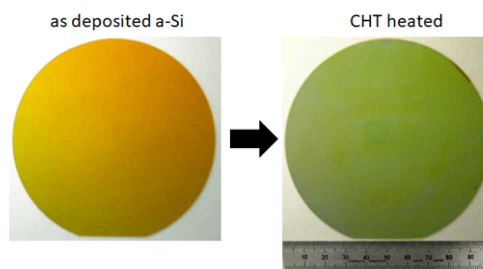

FIGURE 5. (Color online) Photographs of the initial 58-nm thick amorphous and crystallized silicon films by CHT heating.

the microwave power, and that the microwave power in the cavity was almost completely absorbed by the CHT. The calculation supports experimental results of low microwave refection from the cavity and effective heating of the CHT, as shown in Fig. 2.

Figure 4 shows a demonstration of (a) temperature of the CHT controlled using the PID circuit and (b) change in the microwave power. The plan with heating and cooling rates of 20 K/s, and a temperature of 1100 °C was set. The temperature of the CHT observed by the thermometer increased approximately in linear, then kept about 1100 °C for 75 s and then decreased approximately in linear, as shown in Fig. 4(a). The temperature profile complete different from that shown Fig. 2(b) with constant microwave power resulted from the control the microwave power by the PID circuit following the temperature plan, as shown by Fig. 4(b). However, in fact, the heating rate distributed from 0 to 30 K/s, the keeping temperature fluctuated from 1110 to 1100 °C, and the cooling rate distributed from 0 to 20 K/s because the condition of PID control with best time constant has not established yet and the present thermometer has no sensitivity below 550 °C. For all those problems to be solved in a future, this demonstration shows a capability of designing temperature sequence for the CHT heating system.

Figure 5 shows photographs of the initial amorphous (left) and crystallized silicon films (right). The brown color of the initial amorphous silicon was uniformly changed to green yellow by the CHT heating. This means that a phase change was realized uniformly achieved by the heat treatment.

Figure 6 shows the optical reflectivity spectra of the initial amorphous silicon and the silicon film sample heated by the CHT measured at the central region at the top surface. Although the amorphous silicon film had a broad spectrum, the E_1 and E_2 peaks owing to the optical transition in the tetrahedral crystalline band appeared at 370 and 275 nm in the optical reflectivity spectrum of the CHT-heated silicon film sample. Marked changes in the optical reflectivity caused by the optical interference effect between silicon top surface and bottom interface were also observed for wavelength between 400 and 2700 nm. These characteristics indicate that the

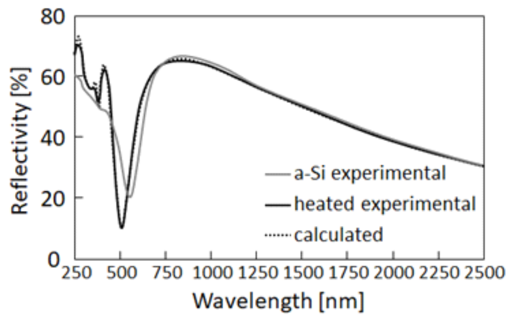

FIGURE 6. Optical reflectivity spectra of the 58-nm-thick as-deposited amorphous silicon film sample and sample heated by the CHT measured at the top surfaces. Calculated curve fitted to the experimental heated sample is also represented by dashed curve.

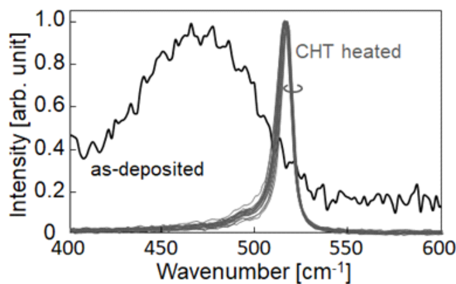

FIGURE 7. Normalized Raman scattering spectra of the 58-nm-thick crystallized silicon films measured at randomly selected 63 points over the whole region and of the as-deposited amorphous silicon film sample.

silicon films were crystallized in the whole thickness region. The experimental optical spectra were analyzed by numerical calculation program [25]–[27]. The dashed curve shown in Fig. 6 was a calculated spectrum with a crystalline volume ratio of 0.92, which well fitted to experimental spectra. The silicon film was well crystallized and the most of disordered region was eliminated.

Figure 7 shows the normalized Raman scattering spectra of the crystallized silicon films measured at randomly selected 63 points over the whole region and of the as-deposited amorphous silicon film sample. The crystallized silicon film had a sharp peak associated with the phonon mode of the crystalline lattice, while the as-deposited amorphous silicon film had a broad peak associated with phonon of disordered bonding structure. The 63 spectra had similar shapes. The peak wavenumber ranged from 514 to 516 cm^{-1}, which was lower than 520.03 cm^{-1} of thermally relaxed crystalline silicon. This indicates the tensile stress existence between the silicon film and quartz substrate. The conventional equation of wavenumber k (cm^{-1}) as a function of stress P (Pa) as $k = 520.03 + 5.2 \times 10^{-9} \times P$ [28] resulted in that the crystallized film was under the tensile stress ranging from 7.7×10^{8} to 1.2×10^{9} Pa. The silicon film was crystallized at a high temperature during CHT heating. The tensile stress is probably generated at the cooling process because silicon has a large thermal expansion coefficient of 2.4×10^{-6} K^{-1} compared with 5.0×10^{-7} K^{-1} of quartz at RT. The full width at half maximum ranged from 7.0 to 9.5 cm^{-1}. Broad tail associated with the phonon mode of nano-crystalline and amorphous structures at around 500 and 480 cm^{-1} were very small. Those results mean that the homogeneous crystalline state was realized.

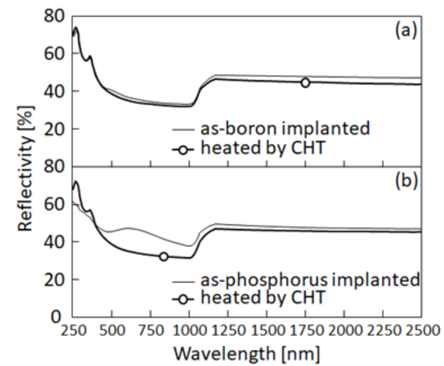

FIGURE 8. Optical reflectivity spectra of (a) as -1×10^{15}-cm^{-2}-boron implanted and CHT-heated-boron-doped surfaces and (b) as -1×10^{15}-cm^{-2}-phosphorus implanted and CHT-heated-phosphorus-doped surfaces.

Figure 8 shows the optical reflectivity spectra of (a) as-boron implanted and CHT-heated-boron-doped-top surfaces and (b) as-phosphorus implanted and CHT-heated-phosphorus-doped-rear surfaces. The heights of E_1 and E_2 peaks caused by tetrahedral crystalline bonding structures in ultraviolet region were slightly low and the reflectivity of infrared was slightly high in the case of as-boron implanted-top surface compared with optical reflectivity spectrum of single crystalline silicon surface. On the other hand, CHT-heated-boron-doped-top surface showed almost the same optical reflectivity spectrum of the single crystalline silicon surface. The optical reflectivity spectrum of as-phosphorus-implanted-rear surface showed very small E_1 and E_2 peaks and a large fringe in the visible and near-infrared region because of optical interference effect with a disordered surface layered structure with different refractive indexes and extinction coefficients from those of single crystalline silicon. On the other hand, the CHT heating markedly changed the optical reflectivity spectrum similar to that of the single crystalline silicon surface with E_1 and E_2 peaks in the ultraviolet region and monotonously decrease in the visible and near infrared region. This means that the CHT heating recrystallized well the phosphorus-implanted-rear-surface regions by heat diffusion via the silicon substrate. The optical reflectivity spectra were analyzed using a numerical calculation program given above [24]–[26] to estimate the in-depth profile of X in the implanted regions.

Figure 9 shows the in-depth profiles of X for (a) as-boron implanted and CHT-heated-boron-doped-top surfaces and (b) as-phosphorus-implanted and CHT-heated-phosphorus-doped-rear surfaces. X was slightly decreased to 0.8 from the surface to 115 nm deep by boron implantation. On the other hand, it was increased to 0.98 by the CHT heating. X was markedly decreased to 0.04 in the top 20-nm region and decreased to 0.6 in the region from 20 to 120 nm deep by

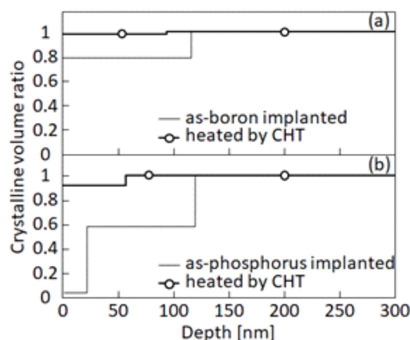

FIGURE 9. In-depth profiles of X of (a) as -1×10^{15}-cm^{-2}-boron implanted and CHT-heated-boron-doped surfaces and (b) as -1×10^{15}-cm^{-2}-phosphorus implanted and CHT-heated-phosphorus-doped surfaces.

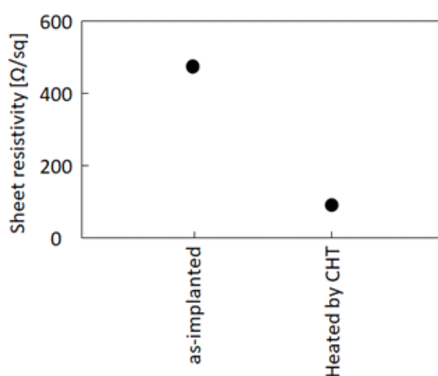

FIGURE 10. Change in the sheet resistivity measured by 9.35-GHz-microwave-transmittance measurement system in dark field for the as-implanted and CHT heated cases.

phosphorus implantation. Heavy phosphorus atoms caused the disordered region in the silicon rear surface. On the other hand, X was markedly increased to 0.92 in the top 60-nm region and 1.0 in the deeper region by the CHT heating. The CHT heating effectively recrystallized the rear surface ion implanted region.

Figure 10 shows change in the sheet resistivity measured by 9.35-GHz-microwave-transmittance measurement system in dark field for the as-implanted and CHT heated cases. A sheet resistivity of 470 Ω/sq for as-implanted case was given by the resistivity of silicon bulk. The sheet resistivity was decreased to 80 Ω/sq by the CHT heating. It means that the implanted boron and phosphorus dopants were activated. The sheet resistivities of as-implanted and CHT heated samples gave the sheet resistivity of 96 Ω/sq for the boron and phosphorus implanted regions. When the effective total depth of boron and phosphorus ion implanted regions at the top and bottom surfaces is assumed as 200 nm, the average resistivity of boron and phosphorus ion implanted region was estimated as 1.9×10^{-3} Ωcm. The low resistivity doped region with a carrier density [28], [30] on the order of 10^{20} cm^{-3} was obtained by the CHT heating.

Figure 11 shows the absolute current density as a function of bias voltage in the dark field. Typical diode characteristic

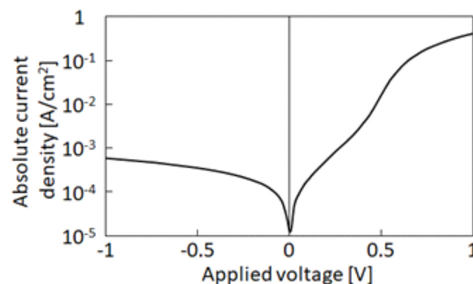

FIGURE 11. Absolute current density as a function of bias voltage in the dark field.

obtained in the dark field measurement indicates pn junction formation associated activation of dopant atoms by the CHT heating.

The results of Figs. 2-11 indicate that the present heating system with the CHT has a capability of application to various heat treatment. High temperature heating of the CHT by low microwave power was demonstrated. Moreover, the CHT with no electrode has an advantage for its application to heat treatment in severe environment for example high humidity atmosphere. The CHT with no electrode will also make it possible to realize simple heating system because no complicated wiring is necessary. Moreover, a capability of lamp with highly thermal proof structure is expected because the junction between lamp materials and the electrode metals has always a serious problem of thermally stress-induced damage.

IV. CONCLUSIONS

A new heating system with a carbon heating tube (CHT) was proposed. The CHT was made with a quartz tube filled with carbon particles and Ar gas. A 60-mm long and 4-mm inner diameter CHT was set in a cavity in which 2.45-GHz microwave was introduced. The semi-spherical cavity closed microwave and made it be effectively absorbed by CHT during multi-reflection of microwave in the cavity with negligible small of microwave reflectance loss. The CHT was effectively heated to a high temperature of 1279 °C and 56 K/s for 33 s microwave irradiation at a power of 200 W. The numerical calculation with three dimensional finite element moment method demonstrated the marked reduction of the electric field intensity to at least 0.1% by introducing the 60 mm long CHT with an electrical conductivity of 55 S/m in the cavity. The PID feedback circuit system with a temperature monitor and a variable power supply demonstrated the capability of the control of the temperature of the CHT. The temperature of the CHT gradually increased to 1100 °C and then also gradually decreased after keeping 1100 °C for 75 s. Crystallization of a 58-nm-thick amorphous silicon thin film formed on 4-inch sized glass substrate was demonstrated by mechanically moving the silicon sample just below the 150-mm long CHT heated at 1100 °C with a microwave power of 400 W. Optical reflectivity spectra measurements revealed that crystallization in the whole film thickness

was achieved. A high crystalline volume ratio of 0.92 was obtained. Raman scattering spectra measurement resulted in sharp peak of crystalline phonon mode with the tensile stress ranging from 7.7×10^{8} to 1.2×10^{9} Pa. Boron and phosphorus atoms implanted with a dose of 1×10^{15} cm^{-2} to the top and rear surfaces were activated by CHT heating at 1100 °C. Recrystallization and the sheet resistivity of 96 Ω/sq of the implanted regions were achieved. J-V measurement resulted in rectified characteristic in the dark field.

REFERENCES

[1] S. Uchikoga and N. Ibaraki, "Low temperature poly-Si TFT-LCD by excimer laser anneal," *Thin Solid Films*, vol. 383, nos. 1–2, pp. 19–24, Feb. 2001.

[2] S. Inoue *et al.*, "Low temperature poly-Si TFT-electrophoretic displays (TFT-EPDs) with four level gray scale," in *IEDM Tech. Dig.*, San Francisco, CA, USA, Dec. 2000, pp. 197–200.

[3] K. Shibata and H. Takahashi, "Active matrix OLED displays with a hight efficiency red emission material," AM-LCD 01, Tokyo, Japan, Tech. Rep., Jul. 2001, pp. 219–222.

[4] M. A. Green, "Commercial progress and challenges for photovoltaics," *Nature Energy*, vol. 1, Jan. 2016, Art. no. 15015.

[5] M. A. Green, K. Emery, Y. Hishikawa, W. Warta, and E. D. Dunlop, "Solar cell efficiency tables (version 48)," *Prog. Photovolt.*, vol. 24, no. 7, pp. 905–913, Jan. 2016.

[6] M. Dahlinger, B. Bazer-Bachi, T. C. Röder, J. R. Köhler, R. Zapf-Gottwick, and J. H. Werner, "22.0% efficient laser doped back contact solar cells," *Energy Procedia*, vol. 38, pp. 250–253, Mar. 2013.

[7] S. M. Sze, "Transferred-electron and real-space-transfer devices," in *Physics of Semiconductor Devices*, 3rd ed. New York, NY, USA: Wiley, 1985, pp. 510–547.

[8] Y. Taur and T. Ning, "Basic device physics," in *Fundamentals of Modern VLSI Devices*, 2nd ed. Cambridge, U.K.: Cambridge Univ. Press, 1998, pp. 9–105.

[9] R. F. Wood and C. E. Giles, "Macroscopic theory of pulsed-laser annealing. I. Thermal transport and melting," *Phys. Rev. B, Condens. Matter*, vol. 23, no. 6, p. 2923, Mar. 1981.

[10] T. Sameshima, S. Usui, and M. Sekiya, "XeCl excimer laser annealing used in the fabrication of poly-Si TFT's," *IEEE Electron Device Lett.*, vol. EDL-7, pp. 276–278, May 1986.

[11] K. Sera, F. Okumura, H. Uchida, S. Itoh, S. Kaneko, and K. Hotta, "High-performance TFTs fabricated by XeCl excimer laser annealing of hydrogenated amorphous-silicon film," *IEEE Trans. Electron Devices*, vol. 36, no. 12, pp. 2868–2872, Dec. 1989.

[12] T. Serikawa, S. Shirai, A. Okamoto, and S. Suyama, "Electrical characteristics of high-mobility fine-grain poly-Si TFTs from laser irradiated sputter-deposited Si film," *Jpn. J. Appl. Phys.*, vol. 28, no. 11, pp. L1871–L1873, Nov. 1989.

[13] S. Higashi, H. H. K. Murakami, S. Miyazaki, H. Watakabe, N. Aando, and T. Sameshima, "Crystallization of a-Si films using thermal plasma jet and its application to thin film transistor fabrication," in *Proc. 1st Thin Film Mater. Devices Meeting*, Nara, Japan, 2004, pp. 25–28.

[14] G. Mannino, "Effect of heating ramp rates on transient enhanced diffusion in ion-implanted silicon," *Appl. Phys. Lett.*, vol. 78, no. 7, pp. 889–891, Feb. 2001.

[15] T. Sameshima and S. Shibata, "Annihilation of photo induced minority carrier caused by ion implantation and rapid thermal annealing," *Jpn. J. Appl. Phys.*, vol. 53, no. 6, pp. 061301-1–061301-6, Jun. 2014.

[16] T. Nakamura, S. Yoshidomi, M. Hasumi, T. Sameshima, and T. Mizuno, "Crystallization of amorphous silicon thin films by microwave heating," in *Proc. MRS Online Library Arch.*, San Francisco, CA, USA, vol. 1666, Nov. 2014, p. A13-09.

[17] S. Kimura, K. Ota, M. Hasumi, A. Suzuki, M. Ushijima, and T. Sameshima, "Crystallization and activation of silicon by microwave rapid annealing," *Appl. Phys. A, Solids Surf.*, vol. 122, pp. 695-1–695-9, Jul. 2016.

[18] M. Yoshikawa *et al.*, "Raman scattering from sp2 carbon clusters," *Phys. Rev. B, Condens. Matter*, vol. 46, no. 11, pp. 7169–7174, Sep. 1992.

[19] T. Sameshima and N. Andoh, "Heating layer of diamond like carbon films used for crystallization of silicon films," *Jpn. J. Appl. Phys.*, vol. 44, no. 10, pp. 7305–7308, Oct. 2005.

[20] T. Miyazaki, G. Kobayashi, T. Sugawara, T. Kikuchi, M. Hasumi, and T. Sameshima, "Carbon heating tube used for rapid heating system for semiconductor annealing," in *Proc. 25th Int. Workshop Active-Matrix Flatpanel Displays Devices (AM-FPD)*, Kyoto, Japan, Jul. 2018, pp. 1–4.

[21] A. O'Dwyer, "Controller architecture," in *Handbook Of PI and PID Controller Tuning Rules*, 3rd ed. London, U.K.: Imperial College Press, 2009, pp. 4–17.

[22] J. H. Richmond, "A wire-grid model for scattering by conducting bodies," *IEEE Trans. Antennas Propag.*, vol. AP-14, no. 6, pp. 782–786, Nov. 1966.

[23] T. Sameshima, H. Hayasaka, and T. Haba, "Analysis of microwave absorption caused by free carriers in silicon," *Jpn. J. Appl. Phys.*, vol. 48, no. 2R, pp. 021204-1–021204-6, Feb. 2009.

[24] T. Sameshima, K. Betsuin, T. Mizuno, and N. Sano, "Minority carrier lifetime behavior in crystalline silicon in rapid laser heating," *Jpn. J. Appl. Phys.*, vol. 51, no. 3S, pp. 03CA04-1–03CA04-6, Mar. 2012.

[25] M. Born and E. Wolf, *Principles of Optics: Electromagnetic Theory of Propagation, Interference and Diffraction of Light*, 6th ed. Cambridge, U.K.: Cambridge Univ. Press, 1980.

[26] T. Sameshima, Y. Matsuda, Y. Andoh, and N. Sano, "Recrystallization behavior of silicon implanted with phosphorus atoms by infrared semiconductor laser annealing," *Jpn. J. Appl. Phys.*, vol. 47, no. 3S, pp. 1871–1875, Mar. 2008.

[27] E. D. Palk, *Handbook of Optical Constants of Solids*. London, U.K.: Academic, 1985, pp. 562–577.

[28] B. A. Weinstein and G. J. Piermarini, "Raman scattering and phonon dispersion in Si and GaP at very high pressure," *Phys. Rev. B, Condens. Matter*, vol. 12, no. 4, p. 1172, Aug. 1975.

[29] J. C. Irvin, "Resistivity of bulk silicon and of diffused layers in silicon," *Bell System Tech. J.*, vol. 41, no. 2, pp. 387–410, Mar. 1962.

[30] K. Ukawa, Y. Kanda, T. Sameshima, N. Sano, M. Naito, and N. Hamamoto, "Activation of silicon implanted with phosphorus and boron atoms by infrared semiconductor laser rapid annealing," *Jpn. J. Appl. Phys.*, vol. 49, no. 7R, pp. 076503-1–076503-7, Jul. 2010.

TOSHIYUKI SAMESHIMA received the M.E. and D.E. degrees from the Department of Science, Shizuoka University, Shizuoka, Japan, in 1980 and 1991, respectively. He is currently a Professor with the Department of Electrical and Electronics Engineering, Tokyo University of Agriculture and Technology. He has published 150 refereed original papers. He holds 110 patents. His research interests include semiconductor device, processing technology, and evaluation analysis. He is a member of the Japan Society of Applied Physics.

TOMOYOSHI MIYAZAKI is currently pursuing the Ph.D. degree with the Department of Electrical and Electronics Engineering, Tokyo University of Agriculture and Technology. He is also a CEO of Techno Research Co., Ltd., Tokyo. His research interests include carbon heating tube process and vacuum technology.

GO KOBAYASHI received the B.E. degree from the Graduate School of Environmental Material Chemistry, Tokyo Denki University, Tokyo, Japan, in 2006.

He is currently an Assistant Manager with the Basic Research Department, ORC Manufacturing Co., Ltd. He holds 50 patents. His research interests include basic chemistry, material chemistry, and new light source development.

TAKUJI ARIMA (M'04) received the M.E. and D.E. degrees in engineering from the Tokyo University of Agriculture and Technology, Tokyo, Japan, in 1999 and 2002, respectively, where he is currently an Associate Professor with the Department of Electrical and Electronics Engineering. He is also a part-time Researcher with the National Institute of Information and Communications Technology, Tokyo. His research interest includes computational electromagnetics and metamaterials. He received the Young Scientist Award from the IEEE Antennas and Propagation Society Japan Chapter.

TOSHITAKA KIKUCHI is currently pursuing the master's degree with the Department of Electrical and Electronics Engineering, Tokyo University of Agriculture and Technology, Tokyo, Japan. His research interest includes carbon heating tube process technology and thesis.

TAKUMA UEHARA is currently pursuing the degree with the Department of Electrical and Electronics Engineering, Tokyo University of Agriculture and Technology, Tokyo, Japan. His research interest includes carbon heating tube process technology and thesis.

TAKASHI SUGAWARA is currently pursuing the master's degree with the Department of Electrical and Electronics Engineering, Tokyo University of Agriculture and Technology, Tokyo. Japan. His research interest includes carbon heating tube process technology and thesis.

MASAHIKO HASUMI received the Ph.D. degree from the Graduate School of Arts and Science, The University of Tokyo, Japan, in 1992. He is currently an Assistant Professor with the Department of Electrical and Electronics Engineering, Tokyo University of Agriculture and Technology, Japan. He has published 40 refereed original papers. His research interests include semiconductor devices, processing technology, and evaluation analysis. He is a member of the Japan Society of Applied Physics and the Physical Society of Japan.

IZUMI SERIZAWA received the M.E. degree from the Department of Electro-Photo-Optics, Tokai University, Japan, in 1988. He is currently the General Manager with the Basic Research Department, ORC Manufacturing Co., Ltd. He holds 100 patents. His research interest includes ultraviolet light source and their application techniques.